

Effect of transient thermal cycles in a supercritical water-cooled reactor on the microstructure and properties of ferritic–martensitic steels

T.C. Totemeier^{*}, D.E. Clark

Idaho National Laboratory, P.O. Box 1625, MS 2218, Idaho Falls, ID 83415, United States

Received 30 January 2006; accepted 20 April 2006

Abstract

Microstructural and mechanical property changes in modified 9Cr–1Mo and HCM12A ferritic–martensitic steels resulting from short-duration thermal transients that occur during loss of feedwater flow events in a supercritical water reactor (SCWR) were studied. Specimen blanks were exposed to reference transients with 810 and 840 °C maximum temperatures using a thermal cycle simulator, and the subsequent microstructure, hardness, and creep-rupture strength were evaluated. Exposure to five consecutive cycles at either temperature resulted in no significant changes – only very slight indications of overtempering. Subsequent study of a wider variety of transient conditions showed that significant ferrite-to-austenite transformation occurred during thermal transients whose maximum temperature exceeded 860 °C, or during transients with holds exceeding 10 s at 840 °C maximum temperature. The subsequent presence of untempered martensite in the microstructure, coupled with severe overtempering, resulted in an order of magnitude decrease in creep-rupture strength at 600 °C. The findings were consistent with measured A_{c1} temperatures for the two steels and the dependence of A_{c1} on heating rate.

Published by Elsevier B.V.

1. Introduction

The supercritical water-cooled reactor (SCWR) concept is being studied as part of the United States Generation-IV advanced nuclear reactor research program [1]. The SCWR extends existing light water reactor (LWR) technology to the higher temperature and pressure supercritical regime, with a commensurate increase in thermal efficiency from 33% to about 45% [1,2]. Supercritical water conditions are cur-

rently used in modern coal-fired power boilers with similar advantages in efficiency [3]. The reference US SCWR design is a large plant utilizing a thermal neutron spectrum, low-enrichment uranium oxide fuel, and light water cooling and moderation. The operating pressure and core inlet/outlet temperatures are 25 MPa and 280/500 °C, respectively. Ferritic–martensitic steels containing 9–12 wt% Cr [4–6], such as modified 9Cr–1Mo (American Society of Mechanical Engineers [ASME] Grade 91) and HCM12A (ASME Grade 122) have been selected as candidate materials for fuel cladding due to their combination of elevated temperature strength, irradiation swelling resistance, and expected resistance

^{*} Corresponding author. Tel.: +1 208 526 3074; fax: +1 208 526 4822.

E-mail address: terry.totemeier@inl.gov (T.C. Totemeier).

to irradiation-assisted stress-corrosion cracking in supercritical water conditions [1]. Ferritic–martensitic steels form martensite upon air cooling and are used in a normalized-and-tempered condition with an initial microstructure of tempered martensite, $M_{23}C_6$ carbides (where M is primarily Cr) along prior austenite and subgrain (lath) boundaries, and in some cases, fine MX carbonitride precipitates (where M is primarily Nb and V and X is C or N) within the laths.

One potential limitation of ferritic–martensitic steels is their microstructural stability and strength in thermal transients which occur in off-normal reactor conditions. Their strength above the final $\sim 750^\circ\text{C}$ tempering temperature is poor, and exposure to such temperatures may result in severe weakening due to dislocation recovery and carbide coarsening, or embrittlement due to untempered martensite formation after exposure to temperatures in excess of the equilibrium ferrite-to-austenite transformation temperature, A_{e1} , which is approximately $800\text{--}820^\circ\text{C}$ for typical ferritic–martensitic steels.

A preliminary safety analysis of the SCWR system [7] identified two events in which the fuel cladding experiences excessively high temperatures: (1) a large break in the feedwater lines (cold-leg, large-break loss-of-cooling accident), and (2) a loss of feedwater flow (LFW). While the first event is a rare, accident event and damage to the fuel is permitted, the LFW event is considered a moderate-frequency event and must not result in fuel damage. The results of numerical modeling of the LFW event have been presented in Refs. [7] and [8]. The maxi-

mum temperature that the fuel cladding reaches and the duration of the thermal transient resulting from a total loss of feedwater were found to depend on the main feedwater pump coastdown time, the scram delay time, and the auxiliary feedwater flow rate. The peak cladding temperature for typical values of these parameters as a function of time during and after the LFW event was calculated and is shown in Fig. 1 as the ‘program temperature’. In this ‘reference case’ the peak cladding temperature is 810°C and the cladding is above the normal operating temperature for approximately 10 s; the remainder of the transient is cool-down to warm standby mode. Note that the 690°C normal cladding operating temperature given in Ref. [7] and Fig. 1 was a preliminary value used for accident simulation; actual cladding temperatures are expected to be approximately 575°C as shown in Ref. [8].

The 810°C peak cladding temperature in the reference case is above the typical tempering temperature for ferritic–martensitic steels and similar to the A_{e1} temperature. The transient thermal cycle therefore has the potential to degrade the properties of these steels, but the effects will be time-dependent due to the diffusion-based nature of tempering and austenite transformation processes. Although the extremely short duration of the transient suggests that the effects will be minimal, a conclusive answer can only be provided by subjecting test specimens to the actual transient and measuring the resulting properties.

This paper reports the results of a two-part study of the effects of LFW thermal transients on the

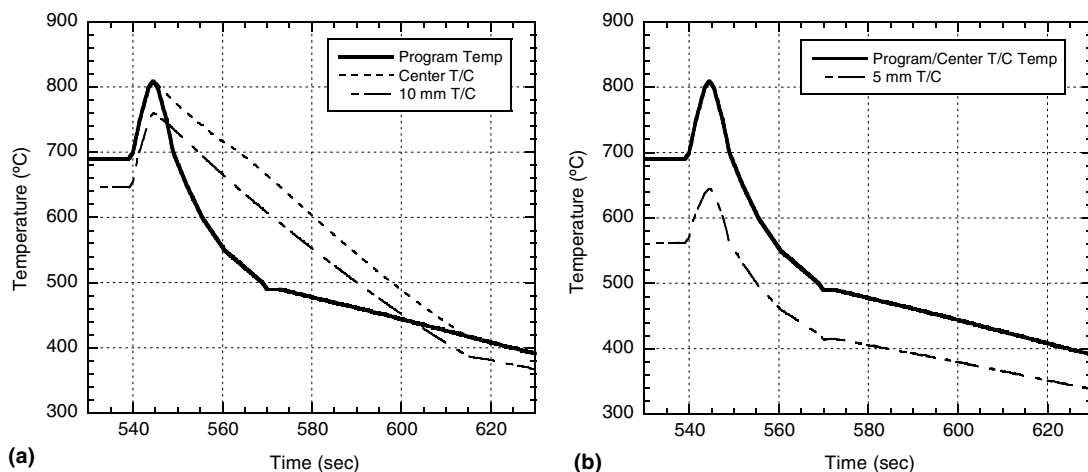


Fig. 1. Plots of thermal transient temperature program, center control thermocouple reading, and monitor thermocouple reading (10 mm from center) as function of time for (a) 50 mm span and (b) 12 mm span between Cu grips in the Gleeble thermal cycle simulator.

microstructure and properties of two typical ferritic–martensitic steels (ASME Grades 91 and 122). A thermal cycle simulator was used in the first part to subject test specimens to the reference thermal cycle with a 810 °C peak temperature and a similar cycle with a 840 °C peak temperature. Changes to the microstructure and creep–rupture strength were evaluated after cycling; as will be shown, no significant changes were observed. A wider range of thermal cycle conditions were evaluated in the second part to identify conditions which did result in marked microstructural alteration, and a limited set of creep–rupture tests were performed to determine the strength of altered structures.

2. Experimental procedures

2.1. Materials

ASME Grade 91 and 122 steels were commercially obtained in a normalized-and-tempered condition. Compositions of the two alloys are given in Table 1. Two heats of Grade 91 steel were used for testing due to a limited quantity of the initial heat (heat-to-heat variations in properties were not intentionally studied). Heat 1 was used to study the 810 and 840 °C reference cycles; heat 2 was used to study the varied thermal cycles. The chemical compositions of the two heats were similar; material from heat 1 was obtained as 13 mm thick plate and material from heat 2 was obtained as 76 mm diameter round bar. The Grade 122 steel was obtained as 30 mm thick plate. Heat 1 of the Grade 91 steel was normalized at 1065 °C, air cooled, and tempered at 790 °C; heat 2 was normalized at 1060 °C, air cooled, and tempered at 745 °C; the Grade 122 steel was normalized at 1050 °C, air cooled, and tempered at 770 °C.

2.2. Thermal cycling

Cylindrical specimen blanks 10 mm diameter and 110 mm long were machined from the stock materi-

als. A Gleeble 3500 (Dynamic Systems Inc., Poetsenkill, NY) thermal cycle simulator was used to subject the specimen blanks to transient thermal cycles similar to that shown as the ‘program temperature’ in Fig. 1. Cylindrical creep and tensile test specimens with 4 mm gage diameter and 17.5 mm reduced section were machined from the cycled blanks. Prior to transient cycling the specimen blanks were heated at 1.7 °C/s to 690 °C (modeled cladding temperature during normal operation) and held for 300 s. Note that the actual cladding operating temperature is expected to be approximately 575 °C; the use of 690 °C instead of 575 °C in the simulated transient is not expected to affect the results due to the very short hold time at 690 °C, which is considerably less than the 760 °C tempering temperature.

A schematic of the Gleeble set-up is shown in Fig. 2. The span between the water-cooled copper grips attached to each end of the specimen blank (which provide resistive heating and conductive cooling) was set to 50 mm. Fig. 1(a) shows the programmed transient temperature profile and specimen temperatures measured in the center of the span and 10 mm away from the center (corresponding to

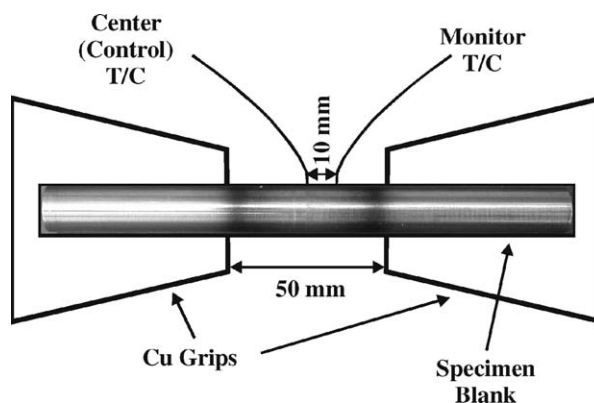


Fig. 2. Schematic diagram of thermal cycle specimen blank illustrating span between the Cu heating/cooling grips and the locations of control and monitoring thermocouples.

Table 1
Chemical composition (wt%)

Alloy	Fe	C	Cr	Mo	V	Cu	W	Ni	Mn	Si	Al	Nb	N	P	S
<i>Grade 91</i>															
Heat 1 (reference cycles)	Bal.	0.10	8.34	0.90	0.22	0.17	–	0.21	0.45	0.28	0.022	0.076	0.048	0.009	0.003
Heat 2 (varied cycles)	Bal.	0.10	8.70	0.90	0.21	0.28	–	0.18	0.33	0.27	0.005	0.074	0.042	0.012	0.004
<i>Grade 122</i>															
	Bal.	0.11	10.83	0.30	0.19	1.02	1.89	0.39	0.64	0.27	0.001	0.054	0.063	0.016	0.002

the edge of the reduced section) for the 50 mm span. The center thermocouple was used for control, and it closely follows the programmed temperature during the heating portion of the transient. The peak temperature 10 mm from the center was about 50 °C lower. Both center and edge temperatures lagged the cooling transient by less than 20 s. As shown in Fig. 1(b), decreasing the span to 12 mm allowed the control thermocouple to exactly match the programmed cooling gradient but resulted in a greater difference between the center and edge thermocouples. An opposite effect was observed when the span is increased (not shown). A 50 mm span was found to provide the best combination of uniform temperature over the test specimen reduced section and good match of the rapid transient heating and cooling rates.

The transient heating and cooling rates in the 840 °C cycle were the same as in the 810 °C reference cycle (24 °C/s); only the peak temperature was changed. The 840 °C cycle was studied in addition to the reference cycle because 840 °C has been identified as a limit temperature for any moderate-frequency transients. Each specimen blank was given 5 consecutive thermal cycles prior to machining and testing in order to simulate the possibility of multiple events occurring over the life of a given fuel element. Between transient cycles the blanks were cooled from the transient end temperature (400 °C) to 100 °C at a rate of 1.7 °C/s, heated to 690 °C at 1.7 °C/s, held at 690 °C for 120 s and then subjected to the transient again.

In the second part of the study a wider range of thermal transient conditions were examined in order to identify transient parameters which resulted in significant microstructural changes for the Grade 91 steel. Specimen blanks were subjected to a series of transient cycles with peak temperatures ranging from 860 to 960 °C and a series of transient cycles with a temperature hold at 840 °C which ranged from 10 to 1800 s. In both series the transient heating and cooling rates were 24 °C/s. Specimen blanks were only subjected to a single transient cycle in the second part of the study.

2.3. Transformation temperature measurement

Phase transformation temperatures in the two steels (Grade 91 heat 2 and Grade 122) were measured using a Theta Industries (Port Washington, NY) vertical differential dilatometer. Cylindrical specimens 12 mm in length and 3 mm in diameter

were heated to 1050 °C in rough vacuum; a Pt standard with the same dimensions was used as the reference. Transformation temperatures were measured at a standard rate of 0.05 °C/s and a rapid rate of 0.8 °C/s. The rapid rate was the closest simulation of the transient heating rate available from the dilatometry equipment. The ferrite-to-austenite transformation temperature A_{c1} was determined from the dilation curves using the technique described in Ref. [9]. For Grade 91 steel the A_{c1} temperatures at the slow and fast heating rates were 827 and 842 °C, respectively, while for Grade 122 steel they were 811 and 841 °C.

2.4. Microstructure and mechanical property evaluation

Microstructures after thermal transient cycling were evaluated using optical and scanning electron microscopy (SEM). Metallographic cross-sections were prepared using standard techniques and immersion etched using either Vilella's reagent or a solution of 30 ml ethanol, 3 g picric acid, 0.6 ml nitric acid, and 1 ml hydrochloric acid. The latter etch was used to reveal carbide precipitates in SEM examination. Carbide size distributions were measured from SEM images of etched sections taken at high magnification (20–40 kX).

Multiple Vickers microhardness measurements with a 500 g load were taken in the center of the heated zone and in an unaffected region of the blank to determine the effect of transient cycling on hardness. Tensile tests were performed at room temperature and creep-rupture tests were performed at 550, 600 and 650 °C. Creep-rupture tests were performed using standard lever-arm machines with averaging, rod-in-tube type extensometers; tests were generally performed to specimen failure. Broken specimens were optically examined for anomalous failure features; none were observed.

3. Results

3.1. Effect of thermal transients on microstructure, hardness, and room-temperature tensile properties

Essentially no effect of five repeated thermal transients at 810 or 840 °C was observed on the microstructure and room-temperature strength of Grade 91 or Grade 122 steels. The etched optical microstructure after cycling to either temperature consisted

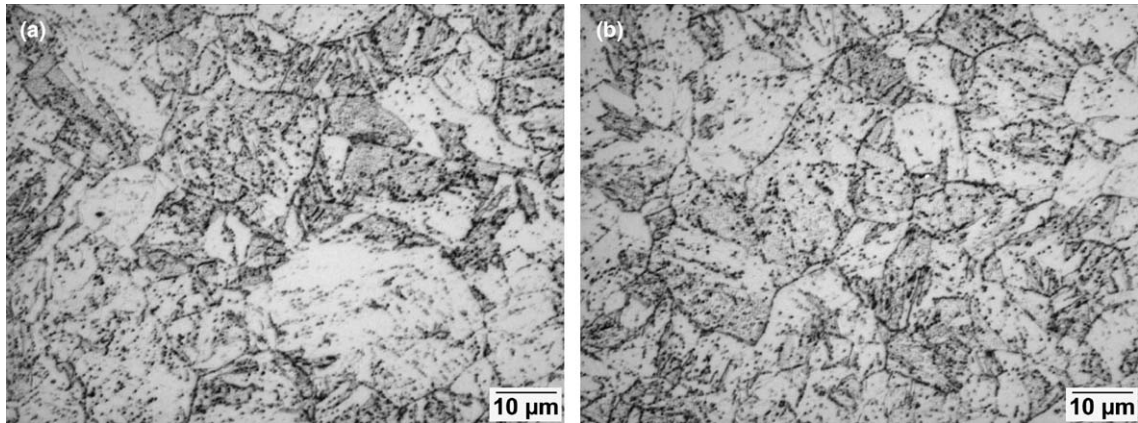


Fig. 3. Optical microstructure of Grade 91 steel (heat 1): (a) baseline prior to cycling, (b) after five transient cycles to 840 °C maximum temperature.

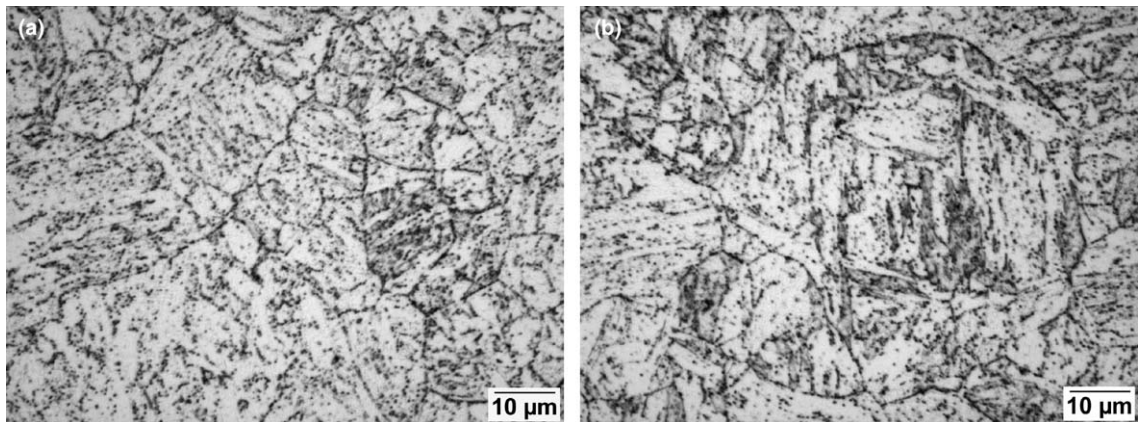


Fig. 4. Optical microstructure of Grade 122 steel: (a) baseline prior to cycling, (b) after five transient cycles to 840 °C maximum temperature.

of tempered martensite indistinguishable from the baseline structure. Fig. 3 shows baseline and 840 °C cycled microstructures for Grade 91; Fig. 4

shows the same for Grade 122. Table 2 summarizes the results of microstructure, hardness, and tensile measurements on baseline and thermally cycled

Table 2
Effect of thermal transient on room temperature microstructure and properties

Alloy	Condition	Mean carbide diameter \pm 95% CI ^a (nm)	Mean microhardness \pm 95% CI (HV ₅₀₀)	Tensile properties			
				Yield (MPa)	UTS (MPa)	Ductility (%)	RA (%)
Grade 91	Baseline	101 \pm 6	225 \pm 5	580	740	27	70
Grade 91	5 cycles @ 810°C	128 \pm 6	222 \pm 2	560	730	27	70
Grade 91	5 cycles @ 840 °C	143 \pm 8	228 \pm 2	– ^b	–	–	–
Grade 122	Baseline	138 \pm 8	247 \pm 2	640	810	25	58
Grade 122	5 cycles @ 810 °C	143 \pm 10	241 \pm 2	610	780	24	60
Grade 122	5 cycles @ 840 °C	140 \pm 8	238 \pm 3	–	–	–	–

^a Confidence interval.

^b Not tested.

specimens. A 95% confidence interval is given for the carbide diameter and microhardness values. Note that this corresponds to the error of mean

value estimate, not the standard deviation (width of distribution peak). Small, but statistically significant, increases in mean carbide diameter were

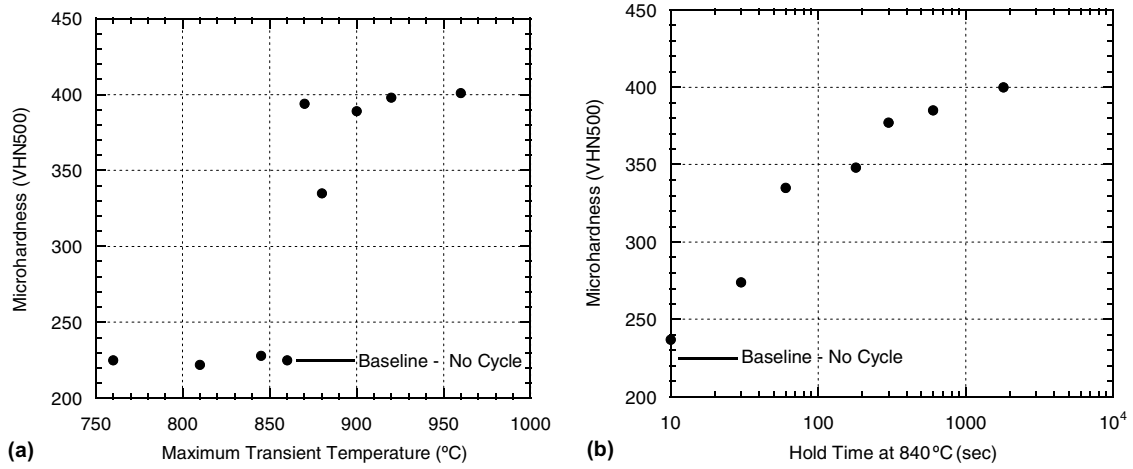


Fig. 5. Variation of Grade 91 (heat 2) post-transient microhardness with (a) maximum transient temperature without hold, (b) hold time at 840 °C maximum transient temperature.

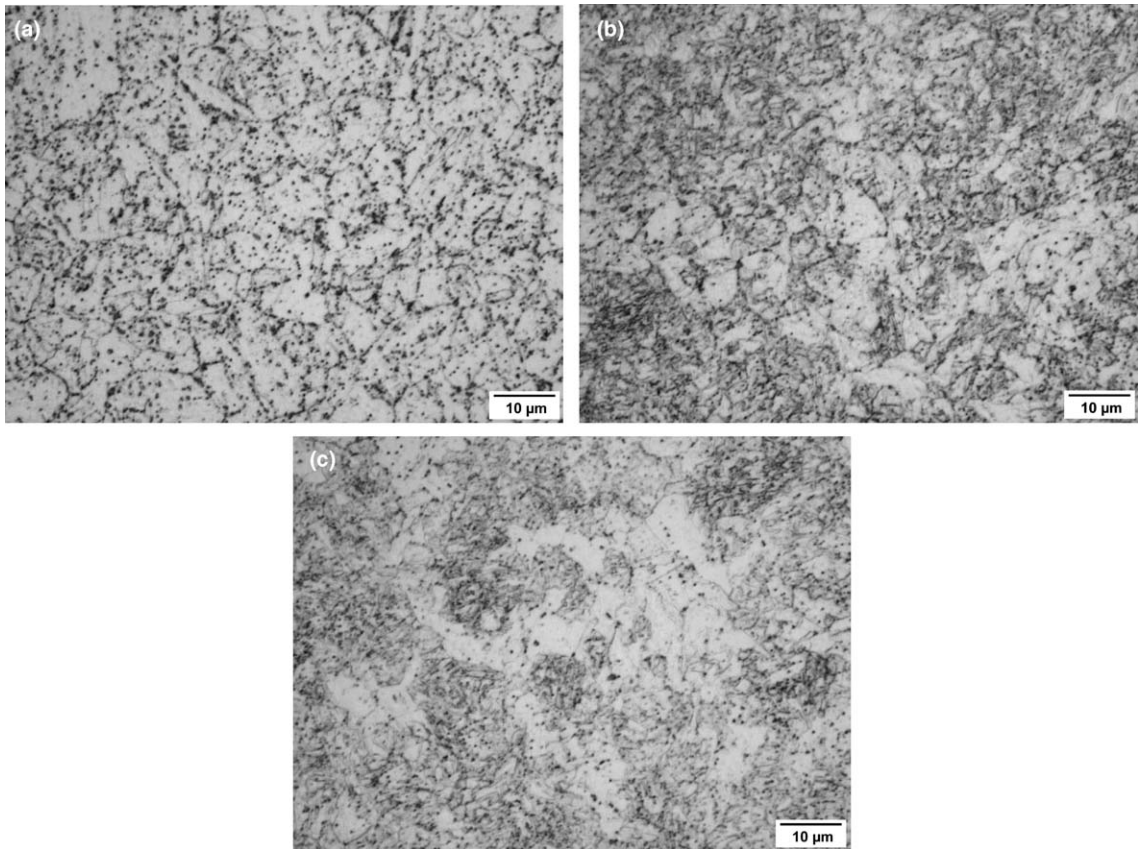


Fig. 6. Optical microstructure of Grade 91 steel (heat 2): (a) baseline prior to cycling; (b) 870 °C maximum transient temperature; (c) 30 s hold time at 840 °C maximum transient temperature. Lightly-etched areas in (b) and (c) are untempered martensite.

observed for Grade 91 after thermal cycling; no significant changes were observed for Grade 122. Conversely, no significant microhardness changes were observed for Grade 91, but a slight decrease was noted for Grade 122 after cycling to 840 °C. Small decreases in yield and ultimate tensile strength with no ductility change were observed in both steels following 810 °C cycling.

The effects of varied maximum transient temperature and hold time at 840 °C transient temperature on the microhardness of Grade 91 steel are shown in Figs. 5(a) and (b), respectively. Also indicated are the pre-cycling baseline hardness values. No change in microhardness was observed for maximum cycle temperatures of 860 °C and below; for transient temperatures above 860 °C the microhardness dramatically increased to a plateau level of 400 VHN₅₀₀. Hold periods at 840 °C greater than 10 s resulted in microhardness that increased with hold duration; a maximum microhardness of 400 VHN₅₀₀ was observed after 1800 s holding at 840 °C. Etched optical microstructures observed after cycling reflected the microhardness changes; significant fractions of untempered martensite were observed for maximum transient temperatures of 870 °C and above and 840 °C hold periods greater than 10 s. Typical baseline and cycled structures are shown in Fig. 6; lightly etched areas in the cycled microstructures are untempered martensite.

3.2. Effect of thermal transients on creep-rupture properties

Fig. 7 shows a comparison of minimum creep rates and rupture lives for thermally-cycled Grade 91 steel to those obtained for the same alloy in a standard heat treatment condition. Minimum creep rates and rupture lives are indistinguishable from baseline and literature data over a wide range of temperatures and stresses. Specimens which were

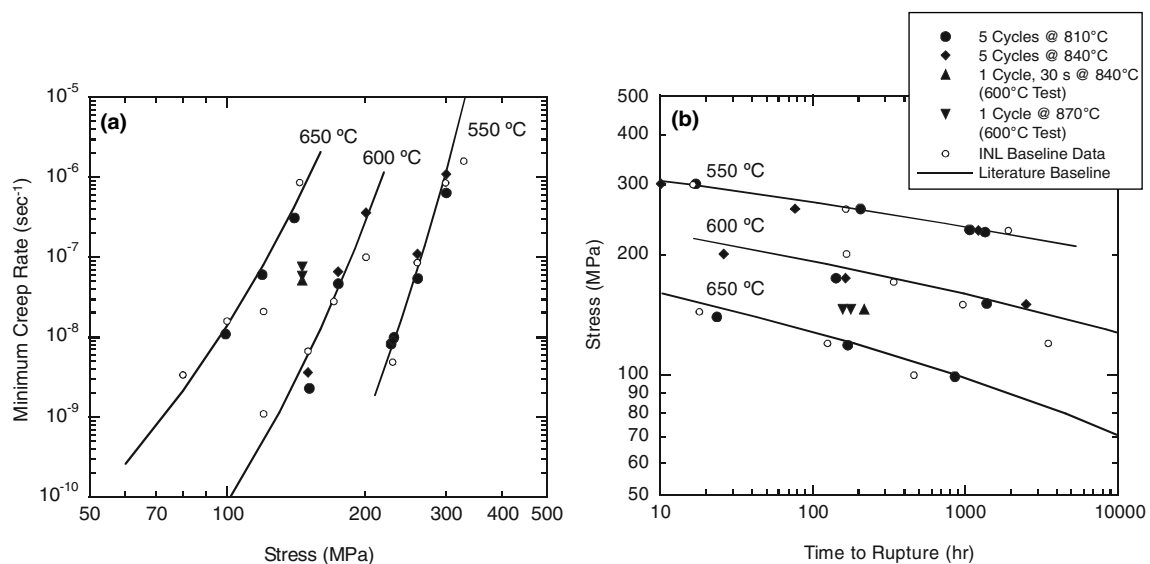


Fig. 7. Comparison of (a) minimum creep rate and (b) rupture life for transient-cycled Grade 91 steel with baseline data. Idaho National Laboratory (INL) baseline data is from Ref. [14], lines representing literature baseline from Ref. [15].

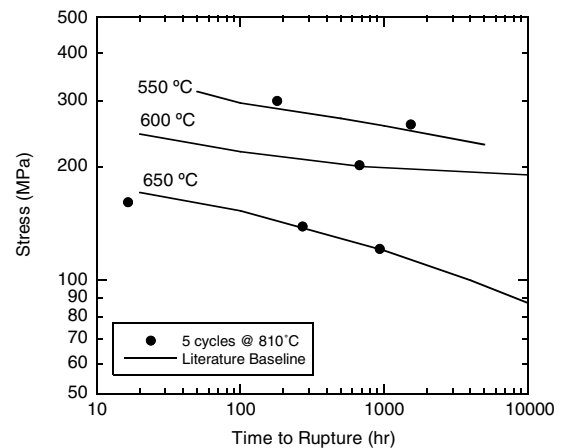


Fig. 8. Comparison of rupture life for Grade 122 steel after transient cycling with lines representing baseline data from Ref. [16].

cycled to 870 °C maximum temperature or with a 30 s hold at 840 °C show dramatically lowered creep strength, slightly greater than a factor of 10 in either minimum creep rate or rupture life at the condition tested, 600 °C and 145 MPa.

Fig. 8 compares rupture life data for cycled Grade 122 steel with literature data – again there is apparently no effect of repeated transients at either 810 or 840 °C. Creep ductilities for both alloys (not shown) after thermal cycling are not different than in a standard heat treatment condition, with typical failure elongations of 25–30% for Grade 91 and 15–20% for Grade 122.

4. Discussion

The results obtained indicate that repeated thermal transients to 810 or 840 °C in a reference LFW event have a negligible effect on the microstructure and properties of Grade 91 and Grade 122 ferritic–martensitic steels. The slight changes observed in mean carbide diameter and room temperature tensile strength are consistent with a slight degree of overtempering with no evidence of martensite formation.

These observations are consistent with the maximum transient temperatures, the rapid heating and cooling rates, and the short transient durations. The 810 and 840 °C maximum transient temperatures do not exceed the A_{c1} temperatures measured for either steel at a heating rate of 0.8 °C/s, which were 842 and 841 °C for Grade 91 and Grade 122, respectively. Since the transient heating rate is considerably greater (24 °C/s), the transformation temperature during the transient will be even higher than those measured (A_{c1} increases with heating rate [9]). The observation of a dramatic increase in hardness for Grade 91 steel when the maximum transient temperature was increased from 860 to 870 °C indicates that A_{c1} for a heating rate of 24 °C/s lies between these two temperatures. Such an increase is consistent with that observed when the heating rate was increased from 0.05 °C/s to 0.8 °C/s. In this case a 16 X increase in heating rate resulted in a 15 °C increase in A_{c1} . The 30 X increase in heating rate from 0.8 to 24 °C/s appears to result in a 20 °C increase in A_{c1} . Because the A_{c1} temperature for ferritic–martensitic steels is roughly proportional to the logarithm of the heating rates [9], these relative increases are consistent.

The very limited degree of overtempering observed during the transient cycles at 810 and 840 °C is due

to the very short time above the standard 760 °C tempering temperature during the transient; approximately 4 s for the 810 °C transient and 7 s for the 840 °C transient. Tempering is a diffusion-based process [10] and time at temperature is required – standard tempering times are greater than 1 h, so it is not surprising that exposure times less than 10 s have little effect on a previously-tempered structure.

Observation of significantly increased hardness and untempered martensite in the microstructure of Grade 91 steel held at 840 °C for times greater than 10 s is also consistent with the measured transformation characteristics. Although A_{c1} for continuous heating at 24 °C/s is considerably greater than 840 °C (860–870 °C as indicated by the maximum transient temperature tests), 840 °C is greater than the equilibrium transformation temperature A_{c1} . The value of A_{c1} measured at the slow heating rate of 0.05 °C/s, 827 °C, can be taken as a reasonable approximation of A_{c1} , and therefore transformation to austenite will occur at 840 °C given sufficient holding time. The kinetics of the transformation are evident in the increasing hardness with hold duration at 840 °C with the transformation apparently complete at 1800 s, as a microhardness equivalent to the plateau level in the maximum temperature transient tests was obtained.

In all cases the cooling rates to 100 °C following the transient were sufficient to produce fully martensitic structures in these air-hardening steels. Very slow cooling below A_{f1} (austenite-to-ferrite transformation temperature during cooling) and above the martensite start temperature would be required to produce ferritic rather than martensitic structures from austenite formed in the transient. Martensite start temperatures are between 350 and 400 °C for the two steels, so cooling to a reactor ‘warm standby’ temperature of approximately 250 °C [7] will result in martensite formation.

The results of these studies confirm that the both the ‘reference’ transient cycle and cycles at the ‘limit’ transient temperature will not be damaging to fuel cladding using either ferritic–martensitic steel. The safety margin is not great, however, as an increase of merely 20 °C above the current ‘limit’ temperature would result in significant microstructural alteration and degradation of elevated temperature strength, as will any small hold duration at the limit temperature (equivalently, ‘rounding’ of the transient peak with significant time above A_{c1} will also cause transformation).

The limited creep-rupture tests performed on Grade 91 steel with microstructure altered by the transient show that the creep rate is increased and the rupture life decreased by an order of magnitude. These reductions were observed for the first transient conditions that caused an observable change – further increases in maximum temperature or hold time above A_{c1} may result in further strength reduction as the fraction of untempered martensite in the structure increases and the untransformed tempered martensite becomes more severely overtempered. These reductions are consistent with other studies of off-normal microstructures in ferritic–martensitic steels [11] – the major problem is that the fine distribution of carbide and carbonitride precipitates essential to the strength of ferritic–martensitic steels [12] is disrupted. The presence of untempered martensite is not only detrimental to elevated temperature creep strength but also low-temperature toughness [13], a characteristic that was not measured in this study.

Transient conditions which do not result in microstructural transformation and loss of strength for other ferritic–martensitic steels (or other heats of the steels studied) will be dependent on the specific transformation characteristics for the steel in question. In an ideal case the maximum ‘off-normal’ transient temperature would lie reasonably below the A_{c1} temperature for the cladding steel. An additional factor which was not considered in this study is the effect of radiation exposure on ferrite to austenite transformation kinetics of ferritic–martensitic steels. Fuel cladding will experience a high radiation dose over its lifetime, and the altered chemistry and stored energy of lattice defects resulting from the irradiation may significantly affect transformation temperatures and kinetics.

5. Conclusions

Microstructural and mechanical property changes in two ferritic–martensitic steels (ASME Grades 91 and 122) resulting from short-duration thermal transients that occur during LFW off-normal events in a SCWR were studied and the following conclusions reached:

1. Exposure to five transient cycles with maximum temperatures of 810 and 840 °C resulted in no significant changes to microstructure, room-temperature hardness, or creep-rupture strength over a wide range of conditions. Very slight indica-

tions of overtempering were observed, but there was no sign of austenite formation during the transients.

2. Significant fractions of untempered martensite were observed in Grade 91 steel after thermal transients whose maximum temperature exceeded 860 °C, or after transients with holds exceeding 10 s at 840 °C maximum temperature. Untempered martensite resulted from ferrite-to-austenite transformation during the transient.
3. The presence of untempered martensite resulting from a thermal transient and subsequent cooling at 1.7 °C/s, coupled with severe overtempering of the remaining structure, was very detrimental to creep-rupture strength – minimum creep rates were increased and rupture lives decreased by an order of magnitude for tests performed at 600 °C and 145 MPa.
4. The findings were consistent with measured A_{c1} temperatures for the two steels and the dependence of A_{c1} on heating rate.

Acknowledgements

The authors would like to acknowledge the assistance of T.C. Morris with metallography and hardness testing and B.C. Perrenoud with thermal cycling. This work was supported by the US Department of Energy, Office of Nuclear Energy, Science and Technology, under contract DE-AC07-05ID14517.

References

- [1] J. Buongiorno, W. Corwin, P. MacDonald, L. Mansur, R.K. Nanstad, R.W. Swindeman, A. Rowcliffe, G. Was, D. Wilson, I. Wright, Supercritical Water Reactor (SCWR): Survey of Materials Experience and R&D Needs to Assess Feasibility, Idaho National Engineering and Environmental Laboratory Report INEEL/EXT-03-00693, 2003.
- [2] K. Ehrlich, J. Konys, L. Heikinheimo, J. Nucl. Mater. 327 (2004) 140.
- [3] F. Masuyama, ISIJ Int. 41 (2001) 612.
- [4] F.B. Pickering, in: A. Strang, D.J. Gooch (Eds.), Microstructural Development and Stability in High Chromium Ferritic Power Plant Steels, Institute of Materials, London, 1997, p. 1.
- [5] P.J. Ennis, A. Czyska-Filemonowicz, Ommi 1 (2002).
- [6] R.L. Klueh, D.R. Harries, High-Chromium Ferritic and Martensitic Steels for Nuclear Applications, ASTM, West Conshohocken, PA, 2001.
- [7] J. Buongiorno, P. MacDonald, Supercritical Water Reactor (SCWR): Progress Report for the FY-03 Generation-IV R&D Activities for the Development of the SCWR in the

- US, Idaho National Engineering and Environmental Laboratory Report INEEL/EXT-03-01210, 2003.
- [8] C.B. Davis, J. Buongiorno, P.E. MacDonald, in: International Conference on Global Environment and Advanced Nuclear Power Plants-GENES4/ANP2003. Kyoto, Japan: Atomic Energy Society of Japan, 2003. Paper 1009.
- [9] C. Garcia de Andres, F.G. Caballero, C. Capdevila, L.F. Alvarez, *Mater. Charact.* 48 (2002) 101.
- [10] G. Krauss, *Steels: Heat Treatment and Processing Principles*, ASM International, Materials Park, OH, 1990.
- [11] M.J. Cohn, J.F. Henry, D. Nass, *J. Press. Vess. – T. ASME* 127 (2005) 197.
- [12] F. Abe, *Mater. Sci. Eng. A* 387–389 (2004) 565.
- [13] G. Cai, H.-O. Andren, L.-E. Svensson, *Metall. Mater. Trans. A* 28A (1997) 1417.
- [14] T.C. Totemeier, J.A. Simpson, in: 4th International Conference on Advances in Materials Technology for Fossil Power Plants. Hilton Head, SC: EPRI, 2004. p. 1269.
- [15] V.K. Sikka, M.G. Cowgill, B.W. Roberts, in: J.W. Davis, D.J. Michel (Eds.), *Ferritic Alloys for Use in Nuclear Energy Technologies*, TMS, Warrendale, PA, 1983, p. 413.
- [16] A. Iseda, Y. Sawaragi, S. Kato, F. Masuyama, in: *Creep: Characterization, Damage and Life Assessments*, ASM International, Materials Park, OH, 1992, p. 389.